WARSAW UNIVERSITY OF TECHNOLOGY Index 351733
FACULTY OF CIVIL ENGINEERING
COMMITTEE FOR CIVIL AND WATER ENGINEERING
POLISH ACADEMY OF SCIENCES ISSN 1230-2945

DOI: 10.24425/ace.2022.143036

ARCHIVES OF CIVIL ENGINEERING

Vol. LXVIII ISSUE 4 2022

© 2022. Maciej Cwyl, Stanisław Wierzbicki, Rafał Michalczyk.

pp. 237 – 252

This is an open-access article distributed under the terms of the Creative Commons Attribution-NonCommercial-NoDerivatives License (CC BY-NC-ND 4.0, https://creativecommons.org/licenses/by-nc-nd/4.0/), which permits use, distribution, and reproduction in any medium, provided that the Article is properly cited, the use is non-commercial, and no modifications or adaptations are made.

Research paper

Laboratory tests and numerical analysis of façade sub-structure made of austenitic steel

Maciej Cwyl[1], Stanisław Wierzbicki[2], Rafał Michalczyk[3]

Abstract: This article presents a study of a wall cladding system composed of stainless steel sub-frame and composite, fibre-reinforced concrete cladding panels, which was been installed on a high-rise public building. The study focused on the assessment of strength, safety and durability of design through laboratory tests and numerical analyses. The laboratory tests were conducted using a threedimensional tests stand and a full-scale mock-up of the wall cladding system built at the laboratory using the actually used materials and cladding panels. The boundary conditions and the test loads corresponded to the values of actions determined during the engineering phase of the high-rise building under analysis. Noteworthy, wind actions were verified by supplementary wind tunnel testing. In addition, the stainless steel was also tested to determine the strength properties of the material actually used in construction. These test were carried out just before commencement of the curtain wall installation. The 3D model was constructed with the application of the finite element method (FEM) to obtain adequate representation of geometry, material performance and structural behaviour of the analysed wall cladding system. Particular attention was paid to determination of the parameters defining the behaviour of the cladding system sub-frame from the angle of plastic deformations of the stainless steel and the resulting failure mechanisms of the members of the structure itself. To this end, the stainless steel was subjected to appropriate performance tests to determine material properties including the values of the proportionality limit and yield strength.

Keywords: frame cladding system, fibre reinforced concrete panel, stainless steel, FEM, laboratory testing of wall cladding systems, discrete model of wall cladding system

[1]PhD., Eng., Warsaw University of Technology, Faculty of Civil Engineering, Al. Armii Ludowej 16, 00-637 Warsaw, Poland, e-mail: maciej.cwyl@pw.edu.pl, ORCID: 0000-0002-2894-7840
[2]PhD., Eng., Warsaw University of Technology, Faculty of Civil Engineering, Al. Armii Ludowej 16, 00-637 Warsaw, Poland, e-mail: stanislaw.wierzbicki@pw.edu.pl, ORCID: 0000-0002-7076-0641
[3]PhD., Eng., Warsaw University of Technology, Faculty of Civil Engineering, Al. Armii Ludowej 16, 00-637 Warsaw, Poland, e-mail: rafal.michalczyk@pw.edu.pl, ORCID: 0000-0001-6499-3812

1. Introduction

In the recent years, it has been seen major developments in the field of public building construction as regards architecture and construction technology. These developments are particularly pronounced in the case of exterior wall cladding systems combining the most recent materials with structural and functional design options [1–3]. In this application, new materials such as polymers, composites, special glass panels, aluminium alloys and modern stainless steels are used alongside conventional construction materials [10,14]. The support systems are, quite often, complex spatial frames designed for structural sealant or point attachment of cladding, to ensure safety of use, accommodate thermal movements and rheological effects, [13]. In this way, the cost of façade work may even exceed 50% of the base building construction cost. The main role of the curtain wall structure is to safely transmit all the relevant permanent and environmental loads acting on the wall cladding system [3, 4]. Presently, in order to meet the high functional and structural requirements, cladding systems are built of several different materials that interact as part of the curtain wall structure [5–7].

The laboratory tests and numerical analyses presented in this article relate to a new wall cladding project, currently under construction, in which cladding is made of corrugated polypropylene fibre reinforced architectural concrete (FRC) panels. The panels were 2.2×1.0 m by 12.0 cm thick in size. The support structure was a stainless steel sub-frame, fixed to the reinforced concrete structure of the building. The test specimen was a full size mock-up of the wall cladding system built with the same parts and materials as used originally in the construction of the building facade. In addition, in order to reflect the actual parameters of the installed curtain wall, the real life installation conditions were simulated and the installers actually involved in the work were employed. The primary aim of this approach was to appropriately reflect the conditions, in which the welded connections were made and concrete cladding panels were attached to the stainless steel sub-frame. The mock-up was subjected to loads determined on the basis of the design assumptions and the relevant construction codes. Cyclic loading test was also carried out in which the total number of 10^4 variable load cycles were applied onto the specimen to check its fatigue performance. In addition the stainless steel of the sub-frame was tested for strength. The laboratory tests were complemented by FEM analyses carried out on the mock-up comprising the steel sub-frame and the concrete cladding panel. Numerical analyses were also carried out for the individual steel brackets to determine the level of safety offered by them, both in terms of ultimate strength and serviceability limits (a detailed analysis of the structural details will be presented in a separate article). Particular attention was paid to analysis of rheological phenomena occurring at higher stress levels [8, 9]. The importance of this analysis stems from the fact that throughout the service life the components of the analysed wall cladding system will be subjected to the dead load of the concrete cladding panels, which constitutes a major long-term action imposed on the sub-structure.

www.czasopisma.pan.pl PAN www.journals.pan.pl
POLSKA AKADEMIA NAUK

2. Experimental study

2.1. Test stands

The tests described in this article were carried out on two test stands. The first of them (test stand No. 1 – Fig. 1a was the primary test stand used for testing sections of the wall cladding system brought from the construction site of the building under construction. The second one (test stand No. 2 – Fig. 1b was used for testing properties of the stainless steel, including yield strength and E-modulus and, last but not least, for assessment of rheological effets.

(a) (b)

Fig. 1. Overview of the two test stands: No. 1 (a) Basic test stand for façade elements
No. 2 (b) Steel parameters test stand

The main part of the spatial test machine in the test stand No. 1 (Fig. 1a) was a compression tester (press) with a horizontal cylinder that applied a test force at the level of ±1000 kN. The working width was about 3.5 m and the support arms were spaced by 1.2 m. The tester was operated by control software which allows setting the values of compression or tensile forces and generate cyclic variable loads simulating the action of wind on the concrete cladding panels. The test frame was used to support the tested sub-frame composed of HEA160 I-beams and 180×10 square hollow sections made of S235 steel – Fig. 2. The test frame simulated rigid supports of the building frame and allowed testing of several portions of the wall cladding system in turns with the purpose to obtain repeatability of the test results.

In addition, two concrete panels were also installed and tested side by side, representing a portion of the real curtain wall as installed on the building. These two panels were 1.0 × 0.5 m and 0.68 × 0.5 m in size (Fig. 3), weighing 82.5 kg and 56 kg respectively.

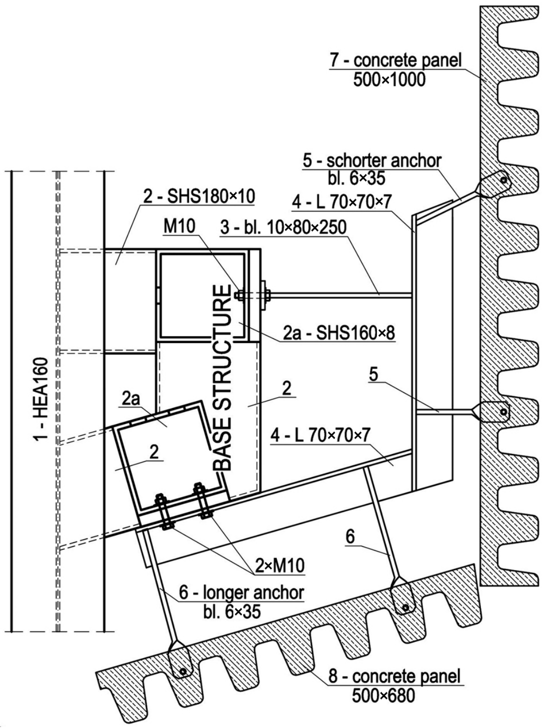

Fig. 2. Schematic representation of the tested mock-up

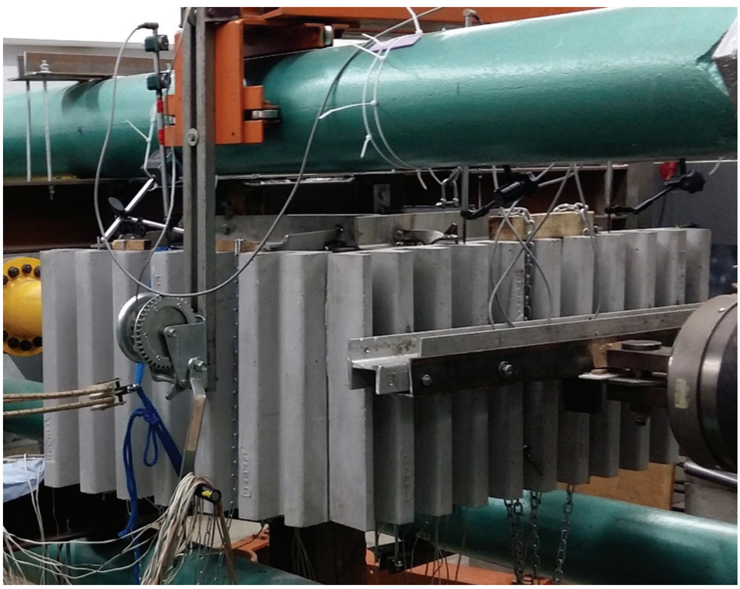

Fig. 3. Overview of the curtain wall mock-up installed in the test stand

The tested sub-frame was made of stainless steel grade 1.4301, the same as the steel of the sub-frame originally installed on the building.

The sub-frame supporting the cladding panels (Fig. 2) was composed of three types of members – bolted 6×35 flat bar, $L70 \times 70 \times 7$ equal leg angle and $10 \times 80 \times 300$ flat bar (all dimensions in mm). The concrete cladding panels were attached to the steel sub-frame with 6 mm steel bolts/ pins. Each panel rested on two anchors and at the top was connected with the next two anchors. The bottom connection prevented relative movement of the bolts and the concrete panel due to a secure connection between the bolts and the panels by epoxy resin. The upper connection between the bolts and the concrete panel was made using plastic sleeves without the use of any adhesive compound. This arrangement allowed free vertical movement of the bolts in relation to the concrete panel. The anchors were connected to the horizontal angle leg with a ca. 3 mm thick fillet weld. The vertical leg of the angle section was, in turn, connected with $10 \times 80 \times 300$ flat bars which are welded to it and attached to 180×10 hollow sections or welded directly to HEA160 beams transmitting the whole amount of load onto the test frame. The fixing arrangement of the concrete cladding panels is represented schematically in Fig. 3. The studied aspects included behaviour of the components under variable cyclic loading that could cause fatigue of the material. The tested mock-up was subjected to loading by vertical and horizontal forces corresponding to the actual loads acting on the analysed curtain wall.

The horizontal forces simulated the action of wind and the vertical forces simulated the dead load of the cladding panel hanging on the building structure. The horizontal forces were applied by movements of the strength tester cylinder with controlled force and also the amount of displacement. Variable loads simulating the action of wind were applied at a frequency of one cycle per 6 seconds and the results were recorded at ca. 0.2 sec. intervals. The fatigue test lasted for 70.7 hours and during that time the total number of 42,000 cycles were applied. The amount of load reflected the difference between 40% of the characteristic positive wind load (pressure) of 1.4 kN/m^2 and 60% of the characteristic negative wind load (suction) of 2.2 kN/m^2. The action of wind was determined on the basis of [11] and considering the results of the wind tunnel test of the building mock-up. The load generated by the cylinder was applied on the concrete panels through a beam laid at the mid-height of each panel to obtain the same load distribution on the two panels. This loading was effected by resting the concrete cladding panels on the anchors and placement of steel plates to obtain the desired amount of load. The 1.00×0.5 m concrete panel was loaded by hanging steel plates weighing 235 kg. The 0.68×0.50 m panel, in turn, was extra loaded by hanging 160 kg plates. Thus the amount of vertical load equalled the weight of the cladding panels increased by a factor of 1.35 (partial safety factor).

Placement of the sensors on the tested elements is shown in Fig. 4 and in Fig. 5. The testing was divided in two stages. In the first stage, the data were gathered by one dial sensor, five inductive sensors (CI1–CI5) and ten strain gauges (T1–T10) and in the second stage additional sensors were placed, including seven strain gauges (T11–T17) and one inductive sensor (CI6). Additional symbols were used to mark the sensor as down (d) or up (g). In the latter stage of testing, the upper bolts were stiffened by welding them to the flat bar anchors. The purpose was to reduce rotation of the bolts in the anchors that secured the upper part of the panel.

www.czasopisma.pan.pl PAN www.journals.pan.pl
POLSKA AKADEMIA NAUK

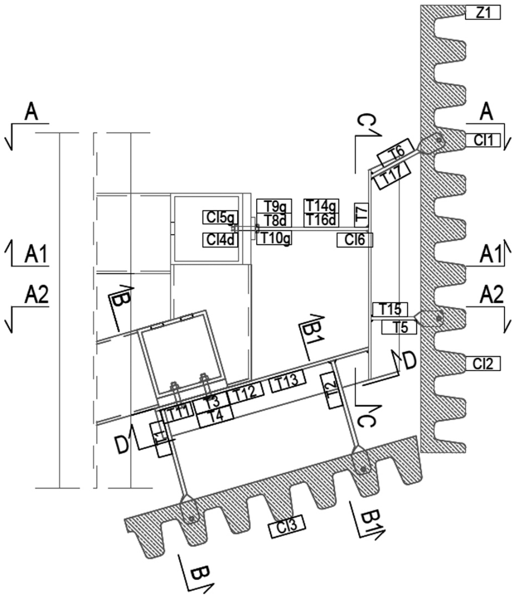

Fig. 4. Placement of inductive sensors (CI) and strain gauges (T) – top view

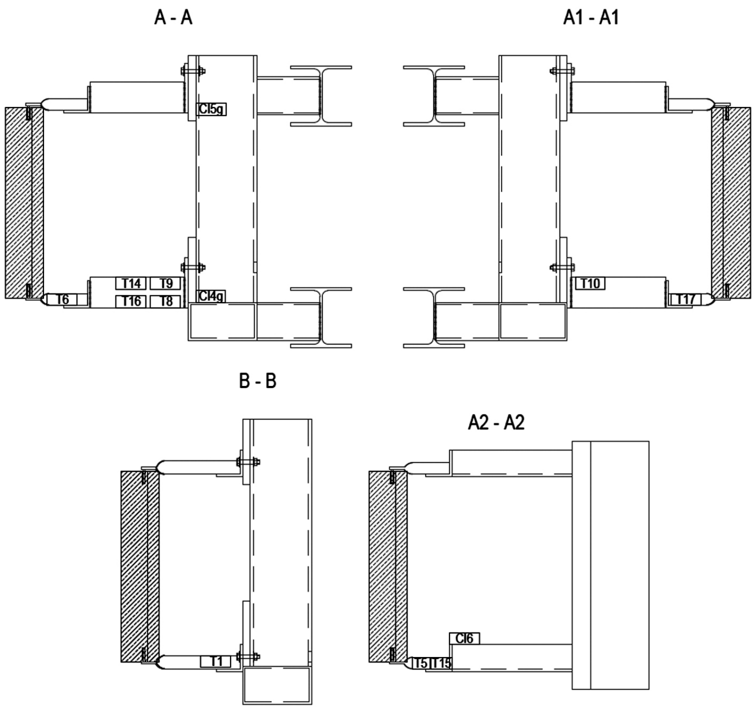

Fig. 5. Placement of inductive sensors (CI) and strain gauges (T) – cross-sections

www.czasopisma.pan.pl PAN POLSKA AKADEMIA NAUK www.journals.pan.pl

The test stand No. 2 (Fig. 1b) was used for testing the stainless steel of the brackets and the results were subsequently used in the numerical analysis of the curtain wall sub-frame components. INSTRON 5567 strength tester was used in the tests. The displacement rate was set on the strength tester at 10 mm/min. The tested items were obtained from the sub-frame angles and the brackets (flat bars) holding in place the concrete cladding panels. The total number of 15 stainless steel samples were tested in order to determine the yield strength at 0.2% strain (further called offset yield strength) and the E-modulus. The obtained values were used to derive the tensile stress-strain curve, subsequently used for numerical modelling of the steel sub-frame components. The test results are presented in Section 2.2.

2.2. Tests results

The steel grade specified in the design documents was 1.4301 austenitic steel, a material with nominal offset yield strength of 210 MPa. At high stress levels, the behaviour of this material is characterised by a strongly nonlinear sigma-epsilon characteristic, as the performance tests have demonstrated. Hence, the design in which this type of steel is specified must ensure that the generated stress levels do not exceed the proportionality limit. Figure 6 gives a reference tensile stress-strain curves of different steels, including austenitic steel, which was the material of the tested curtain wall sub-frame components.

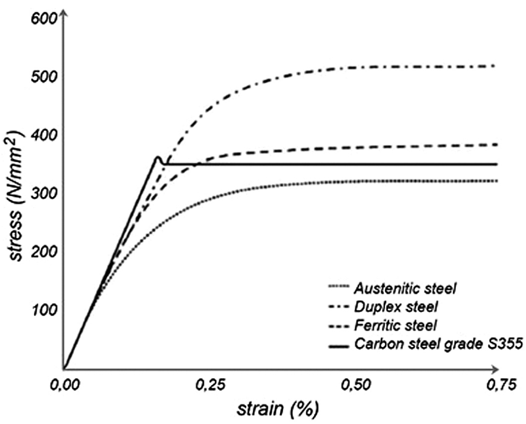

Fig. 6. Stress-strain curves of stainless and carbon steels

For steels whose stress-strain curve does not have a clear yield plateau, offset yield strength is taken at 0.2% strain. However, in the case of austenitic steel, at this level the stress-strain curve already exhibits considerable slanting, associated with plastic strain. Considering this behaviour of the material in question, one should try to reduce the levels of stress generated in the components made of such steel, especially in the case of large permanent loads, by which we mean loads generating stresses in excess of the proportionality limit.

www.czasopisma.pan.pl www.journals.pan.pl

The main tests were carried out on the test stand No. 1. Considering the cyclic nature of loading and a high rate of their variation, the results were recorded at small, i.e. 0.2 sec. intervals. The points for measuring the displacements and strains were planned so as to provide a true picture of the behaviour of the structure and its condition at the key points of the tested elements. Figure 7 represents the characteristic failure mechanisms for the tested curtain wall components.

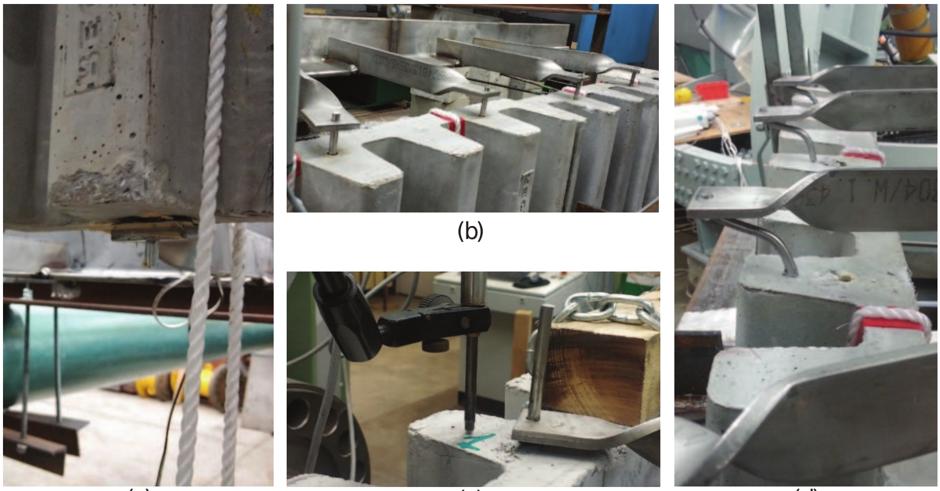

(a) (c) (d)

Fig. 7. Failure modes of the curtain wall components: fracture of mortar where the panel rests on the anchor (a), steel bolts forced out of the concrete panels (b), bolt forced out of the flat bar anchor (c), bolts forced out and bent thereafter (d)

Figure 7a shows brittle fracture failure of a synthetic resin adhesive layer bonding the concrete panel with the steel surface of the curtain wall anchor bracket. This failure was caused by rotation of the support elements due to bending of the bracket under the concrete panel weight. The test lasted for 7–14 days in order to observe long-term behaviour of the structure and pinpoint this failure mode.

Figure 7b shows the top bolts connecting the concrete panels with anchor bars forced out due to excessive deflection of the steel sub-frame under the concrete panels dead load. This is particularly hazardous to the top anchors of the concrete cladding panels which do not bend like other brackets. This situation will pose a problem also in places where lighter panels are positioned over heavier ones, this leading to greater deflections of the supporting anchors.

A slightly different failure mechanism is presented in Fig. 7c. Here we can see the forced out bolt that fixed the concrete panel to the flat bar anchor. This failure mode was observed in the test with cyclic loading with wind suction and pressure applied on the concrete panel, which made the bolts spontaneously slide out of the pockets.

Figure 7d shows a forced out and bent steel bolt of the upper connection between concrete panel and steel sub-frame. This picture shows the connection failure mechanism, which was recorded with the load level exceeding by 30% the design wind pressure of the tested cladding panels. Lack of any major damage (cracks and spalling) of the installation holes in the concrete panels means that despite considerable deformations of the bolt that had slid out of the pocket, the pocket itself retained its capacity to withstand loads.

Besides observation of the failure mechanisms, the laboratory tests allowed recording of displacements and strains in the tested curtain wall section. Fig. 8 shows an example record of displacements as a function of time.

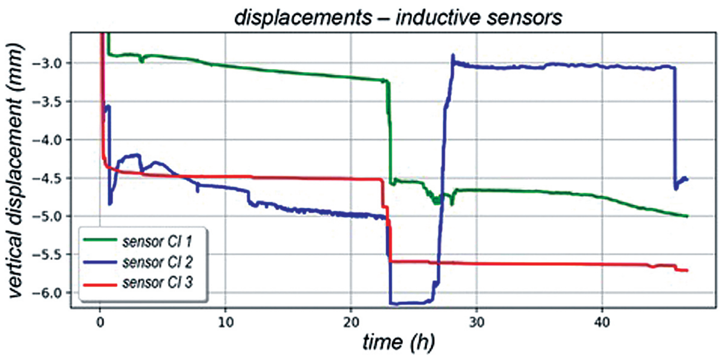

Fig. 8. Example displacement-time graph for the selected inductive sensors

The graph shows displacements due to the deadweight of the cladding panels (stage 1 – the first 24 hours) and the deadweight combined with a horizontal load simulating the action of wind (stage 2 – the next 24 hours). Attention is drawn to the lack of any levelling off of the displacements values from the inductive sensors, confirming the accuracy of the above description of the behaviour of stainless steel subjected to high stress levels. The sudden drop in the value from the inductive sensor No. 2 (blue line) was caused by a temporary change to the loading/ measuring process.

The above-described behaviour of the tested element was confirmed by the strain values obtained with the strain gauges – Fig. 9. The graphs also show an abrupt increase in the

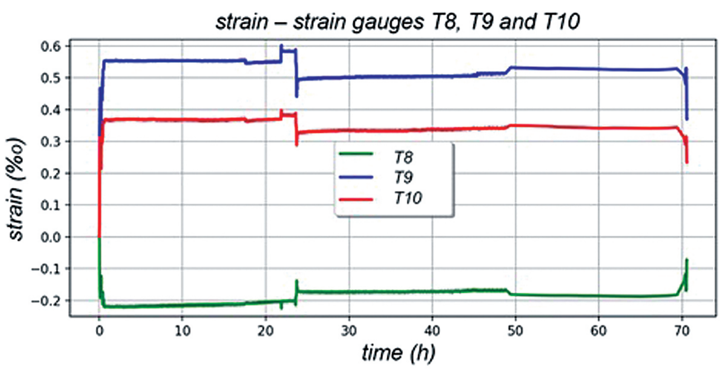

Fig. 9. Example strain plot vs. time for selected strain gauges

measured values after about 24 hours due to the introduction of an additional load to simulate the action of wind on the curtain wall. In the next hours small increases were observed, attributed to plastic flow of the material in question.

2.3. Properties of concrete and austenitic steel

The properties of the stainless steel of the curtain wall sub-frame were determined through appropriate performance tests which provided the data for deriving the constitutive model of the sub-frame steel. In order to appropriately represent the behaviour of steel elements over the whole load range it is essential to determine the non-elastic properties of steel, Fig. 10.

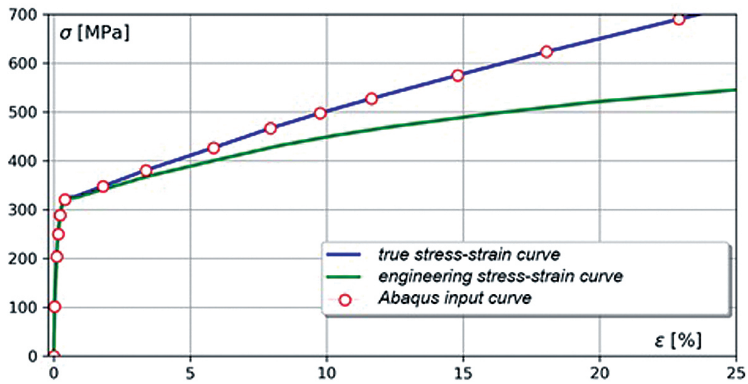

Fig. 10. Averaged stress-strain curves for steel grade 1.4301

A clear yield point is a feature of materials whose curve obtained during the static tensile test includes a distinct plastic plateau, i.e. a region of a considerable increase of strain at small variation in the values of stress. Stainless steels do not exhibit such a behaviour, as it has been demonstrated by the results of the tests performed on the sub-frame material under analysis. Also important is the large non-linearity of the stress-strain curve from the point at which the level of stress reached 200 MPa. Hence, the offset yield strength of R_{pl} = 210 MPa was taken for the strength assessment of the analysed material. Table 1 gives the determined values of the properties of the tested steel and the properties of concrete based on the manufacturer's information.

Table 1. Compilation of the mechanical properties of the steel grade 1.4301 and the concrete

Material	E [MPa]	ν	$R_{pl0.2}$ [MPa]
Steel	200,000	0.3	210.0
Concrete	30,000	0.23	–

3. Numerical analysis

In order to carry out a numerical analysis a FEM model was built using geometrical parameters and material properties given in the design documentation of the structure and complemented by the experimental data. The numerical analysis was carried out in ABAQUS [12]. The numerical model assumes that the structure is made of stainless steel and fixed directly to the reinforced concrete walls with mechanical anchors M10 and M8. The analysed assembly was composed of the top frame, identical bottom frame and two FRC concrete panels of 1001×1420 mm and 679×1420 mm in size, designated G46 and G47 respectively. The geometry and the components of the analysed sub-frame and the FRC panels are shown in Fig. 11.

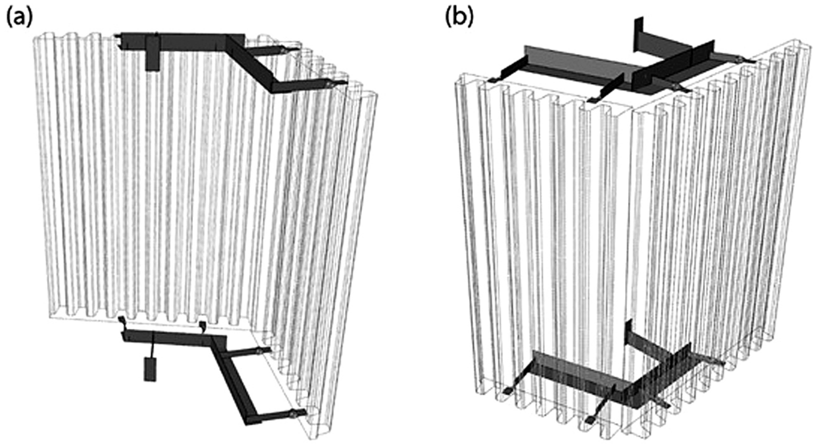

Fig. 11. Rear (a) and front (b) views of the finite-element model

Attachment of the sub-frame to the reinforced concrete wall by means of mechanical anchors was reflected by point elastic support. Also reflected in the model was the method of fixing the panels to the flat bar anchors with bolts, which at the bottom are bonded into the concrete panels and at the top are set in PVC sleeves allowing for vertical movement of these bolts in relation to the panels. The geometry of steel parts was discretized by means of shell elements, specifically 8-node elements with the shape functions described by second degree polynomials and reduced integration, in ABAQUS designated S8R. For the analysed elements the model made of shell elements allows for accurate and quick analysis by modifying the thickness of finite elements and checking of various configurations.

The FRC panels were modelled using eight-node rectangular prism elements. The deformation capacity of the concrete panels was left out of consideration and the role of the concrete panels was limited to loading the tested sub-frame (the panels themselves were analysed in separate calculations). For this reason, only a rough division into elements with linear approximation was applied in this case. The level of grid refinement was based on the results of the analysis of convergence carried out for a few cases to check the effect of the size and number of finite elements on the results of the calculations. Considering the complex stress state, the applied finite elements were smaller, i.e. ca. 5 mm in size. The validation was based on comparing the displacement vs. load relationships obtained through the experimental study and numerical analyses. Consistency was obtained both for the value and the nature of displacements, i.e. the same variation of displacement in both cases. Figure 12 includes the contour map (a) and vectors (b) of resultant displacements.

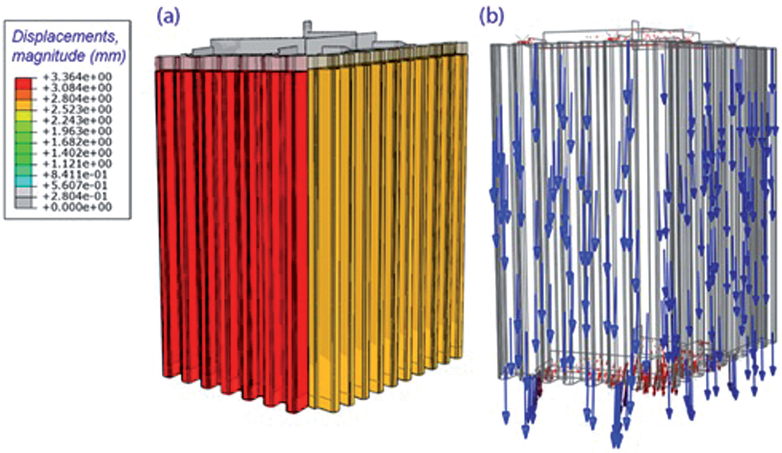

Fig. 12. Displacements: (a) contour map (b) vector map of displacements

The arrangement of the sub-frame results in even downward displacement of the FRC panels. For better illustration of the sub-frame deflections, Fig. 13 shows the resultant deflections of the lower framework (anchors and sub-frame) scaled 20 times and superimposed on non-deformed structure. Figure 14 shows the distribution of von Mises equivalent stresses.

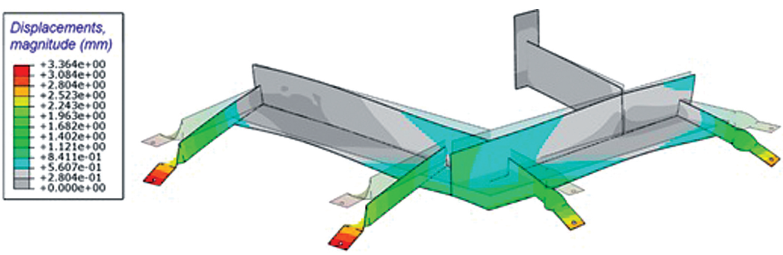

Fig. 13. Resultant displacements of the lower framework – unstrained and strained (scaled 20 times)

For better representation of the stresses two different colour scales were applied. In Fig. 14a the stress level was limited to the offset yield strength of R_{pl} = 210 MPa. In this way, we could estimate where these values were exceeded and pinpoint areas where the material has entered the elastic-plastic region. Figure 14b shows a more detailed stress distribution in yet another colour scale (obtained by limiting the scale to 100 MPa). Loading with panels created stress concentration and high strain areas. The component

www.czasopisma.pan.pl www.journals.pan.pl

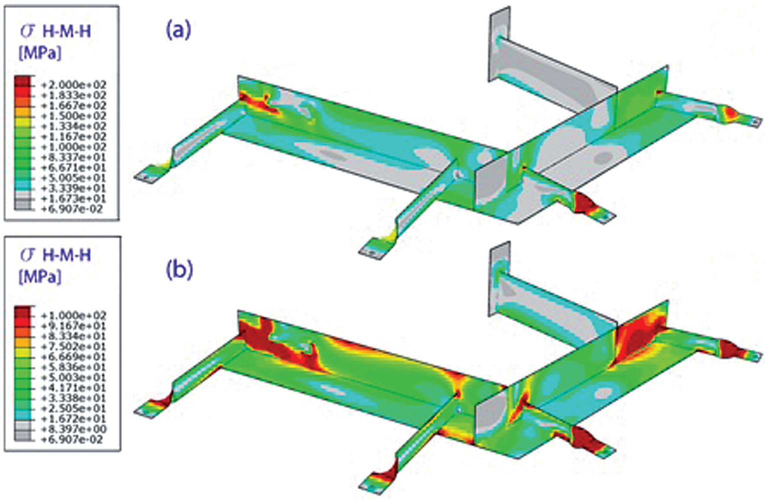

Fig. 14. Contour maps of von Mises equivalent stresses. Two different colour scales were applied

that experienced the greatest load as a result were the shorter anchors. A high stress concentration was also noted at the point of attachment of the outermost, longer anchor. The derived model allows to estimate the effect of various loads on the strain of the anchors and the sub-frame. The presented numerical model provides a true representation of not only the geometry of the analysed structure but also the load (by accurate modelling of the shape of the FRC panels) which allows for considering any effects and loads. Thus, it was obtained a true representation of the phenomena occurring in the elements during service. The modelling methodology was verified with intermediate, validation models and laboratory testing. The following interim conclusions have been derived based on the above-described analyses:

- The displacements (deflections) of the flat bar anchors were not identical and as a result, beside the downward movement the panels also rotate and tilt sideways. Although much less pronounced in the proper model, as compared to the validation model (evident rotation of the panel), this phenomenon can be seen anyway. The amount of deflection depends also very much on the support conditions, namely attachment to the reinforced concrete wall. This translates to sensitivity of the structure to various installation inaccuracies.
- The load imposed by the panels was not distributed evenly on the flat bar anchors. This was caused by different stiffness of different anchors.
- The calculations showed that at some points the equivalent stresses exceeded the plastic strength of 210 MPa. This concerns the zones of attachment of the longer anchor to the angle and fixing of the angle itself, fixing of the shorter anchors and of the end of the shorter corner anchor. Stress concentrations were localised, yet indicate local exceeding of the load limit, particularly undesirable in combination with rheological properties of austenitic steel.

For comparison and verification purposes, a strut-tie model of the curtain wall section was also built. Dimensioning was based on the same assumptions and the experimental study and finite-element analysis. The calculations showed exceeded ULS of the angle and flat bar anchors securing the concrete panels, which is in line with the results of the finite-element analysis. Worth noting is a higher number of zones with exceeded design capacity, which confirms adequacy of all the capacity evaluation methods and hence, the strut and tie model, the most simplified one, should yield the most conservative results.

In addition, analyses considering additional movements of the framing due to installation inaccuracy or movements in the bolted connections. One of the models allows for movement of the sub-frame in relation to anchors by ±1 mm in both vertical and horizontal planes. Horizontal misalignment of anchors is quite probable and thus one should take into account that initially only some anchors will be loaded, and the rest will take on when the frame has "settled down". This is most adverse situation for the framework, largely increasing strength utilisation of some parts thereof. The uneven distribution of load due to inaccuracy of sub-frame assembly and anchor installation results in extra increase of stress in the steel components of the framework and relocation of stress concentration points in relation to the original numerical model. This increase of stress reaches ca. 20–25% in the case of flat bar anchors and ca. 45% in the case of the steel angle member.

4. Conclusions

This article deals with the behaviour of stainless steel in exterior wall cladding systems: curtain walls and rainscreen systems. The study comprised both laboratory tests and numerical finite-element analyses. The finite-element models were validated with the experimental data, which allowed to obtain a better representation of the actual behaviour of the curtain wall subjected to various actions. The following conclusions can be drawn from the results of this experimental study and finite-element simulations:

- The observed sub-frame failure modes concerned primarily the bolts fixing the concrete panels. The 6 mm bolts partly slid out of the holes in the flat bar anchors and then were permanently bent due to eccentric loading. The failure mechanism observed in the case of bolts means the need of particular attention that should be paid to avoid conditions that could result in failure of these bolts.
- The results of the laboratory tests and finite-element analyses confirmed the importance of the flexibility of the steel brackets and stiffness of the sub-frame components. Differences in flexibility resulted in variation in the load distribution and thus also the internal forces and stresses generated in the sub-frame.
- The laboratory tests and numerical analyses confirmed the need to reduce the design stress levels in stainless steel components in view of considerable rheological effects when subjected to long-term loading inducing stress levels that exceed the proportionality limit.

References

[1] C. Bedon, D. Honfi, K.V. Machalická, et al., "Structural characterisation of adaptive facades in Europe – part I: Insight on classification rules, Performance Metrics and design methods", *Journal of Building Engineering*, 2019, vol. 25; DOI: 10.1016/j.jobe.2019.02.013.

[2] C. Bedon, D. Honfi, K. V. Machalická, et al., "Structural characterisation of adaptive facades in Europe – part II: Validity of conventional experimental testing methods and key issues", *Journal of Building Engineering*, 2019, vol. 25; DOI: 10.1016/j.jobe.2019.100797.

[3] C. Bedon, X. Zhang, F. Santos, et al., "Performance of structural glass facades under extreme loads – design methods, existing research, current issues and Trends", *Construction and Building Materials*, 2018, vol. 163, pp. 921–937; DOI: 10.1016/j.conbuildmat.2017.12.153.

[4] *EN 13830:2015 Curtain walling – Product standard.*

[5] M. Cwyl, R. Michalczyk, N. Grzegorzewska, A. Garbacz, "Predicting performance of aluminum – glass composite facade systems based on mechanical properties of the connection", *Periodica Polytechnica Civil Engineering*, 2018, vol. 62, no. 1, pp. 259–266; DOI: 10.3311/PPci.9988.

[6] T.G. Theodosiou, A.G. Tsikaloudaki, K.J. Kontoleon, D.K. Bikas, "Thermal bridging analysis on cladding systems for building facades", *Energy and Buildings*, 2015, vol. 109, pp. 377–384; DOI: 10.1016/j.enbuild.2015.10.037.

[7] AGS, "Elewacje wentylowane, systemy mocowań elewacji, zawiesia sufitowe, nierdzewne konsole do klinkieru, okien, łączniki, systemy mocowań bipv". [Online]. Available: https://ags.org.pl/pl/produkty/. [Accessed: 16. Sept. 2021].

[8] *EN 1993-1-4:2006 Eurocode 3 – Design of steel structures – Part 1–4: General rules – Supplementary rules for stainless steels.*

[9] *Design manual for structural stainless steel*, 4^{th}. The Steel Construction Institute, 2017.

[10] M. Cwyl, I. Dmowska-Michalak, A. Kaczmarczyk, R. Michalczyk, "Laboratory tests and numerical analysis of aluminum helping hand brackets with polyamide thermal break", *Archives of Civil Engineering*, 2022, vol. 68, no. 2, pp. 409–426; DOI: 10.24425/ace.2022.140650.

[11] *EN 1991-1-4 Eurocode 1: Actions on structures – Part 1–4: General actions – Wind actions*. CEN.

[12] Simulia, *ABAQUS v. 6.14; Computer Software and Online Documentation*. Providence, RI, USA: Dassault Systems, 2018.

[13] A. Ambroziak, "Load capacity of steel-aluminium brackets under static and cyclic laboratory tests", *Archives of Civil Engineering*, 2021, vol. 67, no. 2, pp. 85–99; DOI: 10.24425/ace.2021.137156.

[14] G. Schwind, E. Gerasimova, A. Gavamichev, J. Schneider, "Deflection of a cladding panel of fully tempered glass in curtain wall system", *Magazine of Civil Engineering*, 2021, vol. 104, no. 4, pp. 1–15; DOI: 10.34910/MCE.104.3.

Badania laboratoryjne i analizy numeryczne dotyczące konstrukcji elewacji ze stali austenitycznych

Słowa kluczowe: elewacja strukturalna, panel z betonu zbrojonego włóknami, stal nierdzewna, MES, badania laboratoryjne fasad, model numeryczny fasady

Streszczenie:

Współczesne konstrukcje metalowo-szklane notują bardzo intensywny rozwój w obszarze rozwiązań materiałowych, pełnionych funkcji w budynku oraz efektów wizualnych związanych z architekturą realizowanych obiektów. W artykule przedstawiono badania struktury elewacyjnej budynku wysokiego użyteczności publicznej, która została zaprojektowana w postaci rusztu ze stali nierdzewnej i kompozytowych paneli z betonu zbrojonego włóknami. Głównym celem niniejszej pracy była ocena nośności, bezpieczeństwa i trwałości projektowanych rozwiązań, poprzez badania laboratoryjne i analizy numeryczne. Badania laboratoryjne prowadzono na trójwymiarowym stanowisku badawczym, na fragmencie elewacji w skali rzeczywistej, który zbudowano w laboratorium z materiałów i okładzin zastosowanych na realizowanym obiekcie. Fragment elewacji badany w laboratorium został przygotowany przez wykonawców realizujących ocenianą fasadę budynku, co pozwoliło odwzorować standard wykonania taki jak na obiekcie. Warunki brzegowe oraz przyjęte obciążenia odpowiadały wartościom oddziaływań, wyznaczonym na etapie projektowania elewacji wieżowca, przy czym oddziaływania wiatru były weryfikowane uzupełniającymi badaniami w tunelu aerodynamicznym. Przeprowadzono również badania materiałowe stali nierdzewnej, mające na celu określenie rzeczywistych parametrów wytrzymałościowych zastosowanego materiału. Badania przeprowadzono bezpośrednio przed rozpoczęciem realizacji konstrukcji fasady budynku. Wyniki badań eksperymentalnych wykorzystano do walidacji modelu numerycznego odwzorowującego badany fragment elewacji Trójwymiarowy model zbudowano z wykorzystaniem metody elementów skończonych co pozwoliło na odpowiednie odwzorowanie zarówno geometrii, parametrów materiałowych jak i zachowania się analizowanego fragmentu elewacji. Szczególny nacisk położono w artykule na określenie charakterystyki pracy konstrukcji wsporczej elewacji w kontekście odkształceń plastycznych stali nierdzewnej oraz wynikające stąd mechanizmy zniszczenia elementów tej konstrukcji. W tym celu przeprowadzono badania materiałowe stali nierdzewnej w celu określenia parametrów takich jak granica proporcjonalności i granica plastyczności. W artykule wskazano na specyficzny charakter pracy wsporników konstrukcji wsporczej przy uwzględnieniu występowania odkształceń plastycznych charakterystycznych dla stali nierdzewnej. W pracy przedstawiono też mechanizm zniszczenia badanego fragmentu elewacji w przypadku jego przeciążenia.

Received: 2022-06-28, Revised: 2022-09-08